Twisted-wind effect on the aerodynamic force acting on varying side-ratios tall buildings

Yangjin YUAN[1], Bowen YAN [1], Xuhong Zhou[1], Min Wei [1], Qingshan Yang[1]

[1] *Key Laboratory of New Technology for Construction of Cities in Mountain Area (Ministry of Education), School of Civil Engineering, Chongqing University, Chongqing, 400045, China*

SUMMARY:
The influence of side ratio on the aerodynamic performance of tall buildings is investigated by pressure measurement experiments in a mimicked twisted wind field (TWF) with the maximum twisted angle of 30° and its corresponding conventional wind field (CWF). The global wind loads and distribution of local wind forces on the buildings with different side ratios are analyzed in TWF and compared with those in CWF. Additionally, the effect of side ratio on the spatial correlations of aerodynamic forces in temporal and frequency domains and their spectral features are discussed in the two fields. The results show that the aerodynamic forces are largely affected by the side ratio in TWF. The correlation coefficients of local lateral wind force in the TWF are decreased by 0.1-0.4 compared with those in CWF. The trajectory envelopes of the base moment components in lateral and torsional directions are positively inclined, and the building with B/D=2 takes the maximum correlation coefficient. The spectral peak of local torsional forces is diminished with the increasing side ratio in TWF and CWF, and the peak frequency in TWF deviates from that in CWF even though the building is under the equivalent wind direction at some specific elevations.

Keywords: twisted wind field, tall building, side ratio

1. INTRODUCTION

Nowadays, almost all wind-resistant designs of tall buildings are based on a conventional model of the atmospheric boundary layer (ABL) winds, which adopts a fundamental assumption that the wind direction remains invariant with the height. However, it has been recorded in field measurements that the wind speed and horizontal wind direction vary along with the elevation due to the Coriolis force acting on the ABL winds (eg. He et al., 2016; Liu et al., 2018; Shu et al., 2018), namely, the twisted wind field (TWF) (Tse et al., 2016) or veering wind. In addition, it is reported that the TWF might also be produced in mountainous regions due to the effect of topography (Tse et al., 2016). The TWF winds would significantly modify the flow structures around buildings (eg. Zhou et al., 2022) and change the aerodynamic forces on buildings and structures (eg. Liu et al., 2019; Zhou et al., 2021), and the neglect of the twisted effect of wind direction along with the building height might potentially exert unfavored effects on the wind resistant design of tall buildings. Moreover, no current study has systematically addressed the effect of side ratios on the spatial correlation and spectral features of asymmetric wind loads on tall buildings under TWF.

The motivation for the present study is to shed light on the effect of side ratio on the

characteristics of local and global aerodynamic forces on tall buildings under TWF. The correlation of local wind forces at varying building heights and the correlation features among three components of base moments are analyzed and discussed to further elucidate the effects of the side ratio on the aerodynamic forces of the tall building. Additionally, the power spectral and coherence features of fluctuating wind loads are studied to gain more insights into the physical characteristics of the TWF-induced flow and associate fluctuating wind forces at various levels of tall buildings.

2. EXPERIMENTAL SETUPS

In this study, a series of tests were conducted in the Wind Tunnel Laboratory at the School of Civil Engineering, Chongqing University (CQU). This wind tunnel is of an open-circuit type and the dimension of its test section is 2.4m × 1.8m × 15.0m (breadth × height × length). The length scale is 1:500 in the current study. A TWF with the largest twisted angle of 30° was replicated in the wind tunnel using guide vane systems which were designed based on the Ekman spiral (Ekman, 1905). The wind speed (U) and turbulence intensity (I) profiles were generated in the wind tunnel following the power law expressed as $U(z)=U_{ref}(z/z_{ref})^{\alpha}$ and $I(z)=I_{ref}(z/z_{ref})^{-\beta}$, where $U(z)$ and $I(z)$ denote the longitudinal mean wind speed (m/s) and turbulence intensity at the height of z from the ground, U_{ref} and I_{ref} denote the longitudinal mean wind speed and turbulence intensity at the reference height z_{ref} (equal to the height of the building model) and α and β denote the power-law exponent of wind speed and turbulence intensity profiles. A CWF was also simulated with the magnitude of α and β equal to 0.12 and 0.22, which are identical to those for TWF. Fig. 1(a) depicts the mean wind speed profiles $U(z)$ and the turbulence intensity profiles $I(z)$ of CWF and TWF, respectively, and the wind direction profiles $\theta(z)$ are plotted in Fig. 1(b).

A group of rigid building models (M1~M5) with rectangular sections are designed with a height of 1m. As shown in Fig. 2, the section dimension of these models are 0.12×0.12, 0.17×0.09, 0.21×0.07, 0.24×0.06 and 0.27×0.055 (in m), leading to five different side ratios (i.e., B/D approximately equal to 1, 2, 3, 4, and 5 respectively). These building models are designed to provide a roughly identical aspect ratio ($H/\sqrt{BD}$) of 8.2 to eliminate the effect of aspect ratio on the aerodynamic forces. A total of 468 pressure taps were installed on each model. These taps were distributed at 13 levels with 36 taps at each level, as illustrated in Fig. 2.
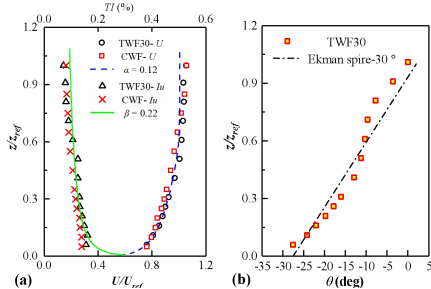

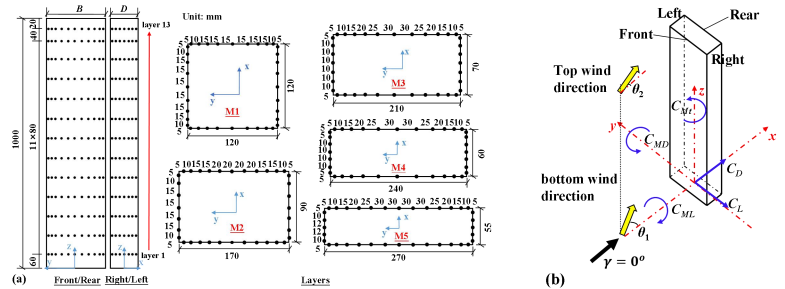Fig. 1 Wind speed and turbulence intensity profile in TWF30 and CWF

Fig. 2(a) layout of pressure taps on the building models, (b) definition of twisted angle and the positive directions for aerodynamic forces

3. RESULTS AND DISCUSSION

3.1 Global and local aerodynamic forces

The characteristics of mean and RMS base moment coefficients are discussed in terms of three orthogonal directions (marked with blue arrows), as demonstrated in Fig. 2 (b). The components of the mean base moment coefficient in longitudinal, lateral, and torsional directions are denoted as $\overline{C}_{MD}$, $\overline{C}_{ML}$, and $\overline{C}_{Mt}$, respectively, and corresponding RMS base coefficients are distinguished with C'_{MD}, C'_{ML}, and C'_{Mt}. It is found that the $\overline{C}_{MD}$ in the TWF30 is decreased compared with that in the CWF, and this observation is more obvious when the wind direction is larger than 30° (Fig. 3). The reduced degree of TWF on $\overline{C}_{MD}$ for the building with $B/D = 3$ is much larger than that with other side ratios.

3.2 Correlation features of local and global wind forces

The correlation coefficients of lateral wind forces among different heights are related to vortex shedding at the side surfaces. In CWF-0°, the correlation coefficient is first increased and then decreased with the increasing side ratio of the tall building and it takes the maximum value as B/D equal to 3. In contrast, in CWF-30°, the correlation coefficients are decreased obviously for different side ratios with the maximum reduction of 0.35. This observation might be attributed to the non-symmetric vortex shedding at the side surfaces in CWF-30°. Additionally, it should be noted that the correlation coefficients in TWF30-0° are reduced by 0.2-0.4 compared with those in CWF-0°, which is induced by the twisted wind direction at the bottom of the building. Analogously, the correlation coefficients in TWF30-30° are decreased by 0.1-0.3 compared with those in CWF-30°, which indicates that the vortex shedding induced by the three-dimensional flows in TWF is much more disordered than that in CWF even though the twisted angle is equal to the wind direction (Fig. 4).
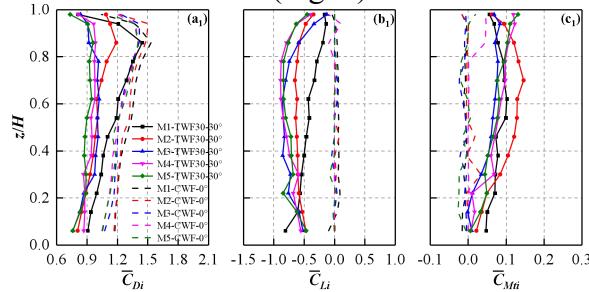

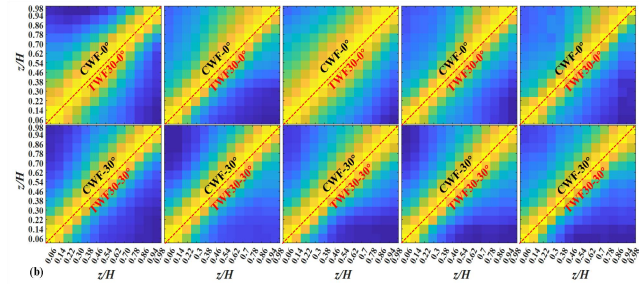Fig. 3 Vertical distribution of mean local forces of the tall buildings under TWF30-30° and CWF-0°.

Fig. 4 Correlation of lateral local wind loads among different layers in CWF-0°, CWF-30°, TWF30-0°

3.3 Frequency-domain features of fluctuating wind loads

The power spectra of local lateral wind forces were obtained for thirteen levels on each of the five building models, and those at z/H = 0.86, 0.7, 0.5, and 0.3 are shown in Fig. 5 to discuss the effect of elevation and side ratio under CWF and TWF. To elucidate the difference and connection of the wind direction and twisted angle, the spectra in CWF-0°, CWF-30°, and TWF30-30° are presented for comparison purposes. The vortex-shedding effects are significant in CWF-0° with only a pronounced peak around the Strouhal frequency. The spectral content beyond the spectral peak is found to decrease obviously at lower elevations for the models with $B/D>1$.
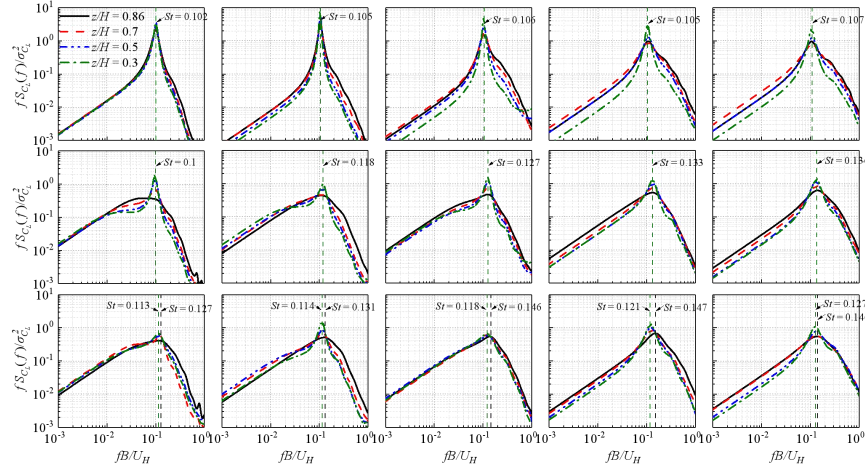
Fig. 5 The PSD of local lateral wind forces of different side ratios in CWF-0°, CWF-30°, and TWF30-30°

4. CONCLUSIONS

In the present study, the TWF30 and corresponding equivalent straight ABL wind field are simulated to evaluate the effects of TWF on the aerodynamic performance of tall buildings with side ratios ranging from 1 to 5.

(1) The $\overline{C}_{Di}$ at the stagnation region is decreased by 11% as the side ratio B/D increased from 1 to 2 due to the effect of TWF, while in the CWF, the effect of side ratios on the local wind forces is slight.

(2) The spatial correlations of local wind forces are reduced by 0.1-0.4 due to the twisted wind direction along the elevation in TWF. The correlations of torsional local wind forces are dramatically decreased with increasing distance due to the combined effect of lateral and longitudinal wind forces in TWF regardless of the side ratio of the tall building.

(3) The vortex shedding frequency in TWF deviates from that in CWF even though the building is under the equivalent wind direction at some specific elevations. The fluctuation contribution of torsional force at the height range of maximum twisted angle is mainly from the vortex-shedding-induced fluctuation of lateral local force for the building with $B/D>3$.

REFERENCES

He, Y.C., Chan, P.W., Li, Q.S., 2016. Observations of vertical wind profiles of tropical cyclones at coastal areas. J. Wind Eng. Ind. Aerodyn, 152, 1–14.

Liu, Z., Zheng, C.R., Wu, Y., Song, Y., 2018. Investigation on characteristics of thousand-meter height wind profiles at non-tropical cyclone prone areas based on field measurement. Build. Environ, 130, 62–73.

Shu, Z.R., Li, Q.S., He, Y.C., Chan, P.W., 2018. Observational study of veering wind by Doppler wind profiler and surface weather station. J. Wind Eng. Ind. Aerodyn, 178, 18–25.

Tse, K.T., Weerasuriya, A.U., Kwok, K.C.S., 2016. Simulation of twisted wind flows in a boundary layer wind tunnel for pedestrian-level wind tunnel tests. J. Wind Eng. Ind. Aerodyn, 159, 99–109.

Zhou, L., Tse, K.T., Hu, G., 2022. Aerodynamic correlation and flow pattern of high-rise building with side ratio of 3:1 under twisted wind profile: A computational study. J. Wind Eng. Ind. Aerodyn, 228, 105087.

Liu, Z., Zheng, C., Wu, Y., Flay, R.G.J., Zhang, K., 2019. Wind tunnel simulation of wind flows with the characteristics of thousand-meter high ABL. Build. Environ, 152, 74–86.

Zhou, L., Tse, K.T., Hu, G., 2021b. Experimental investigation on the aerodynamic characteristics of a tall building subjected to twisted wind. J. Wind Eng. Ind. Aerodyn, 224, 104976.

Ekman, V.W., 1905. On the influence of the Earth's rotation on ocean currents. Ark. Mat. Astr. Fys. 2, 1–52.